Optimization of heat treatment program and effect of heat treatment on microstructure and flexural strength of micro-nano-Li$_2$Si$_2$O$_5$ whisker-reinforced glass-ceramics

Wenli He[1,2†], Chengliang Yao[1,2†], Zihan Zhao[3], Cunren Rong[3], Yanjie Zhang[3], Bing Li[1,2]* and Xiuping Wu[1,2]*

[1]Shanxi Medical University School and Hospital of Stomatology, Taiyuan, China, [2]Shanxi Province Key Laboratory of Oral Diseases Prevention and New Materials, Taiyuan, China, [3]Research Institute of Photonics, Dalian Polytechnic University, Dalian, China

Lithium disilicate (Li$_2$Si$_2$O$_5$, referred as LD) glass ceramics with unique aesthetic properties are ideal dental restorative materials. However, their applications are limited due to the lower flexural strength than polycrystalline ceramics. Herein, micro-nano-LD whiskers were utilized to facilitate the formation of crystallization sites and further growth of crystals in SiO$_2$-Li$_2$O glasses during the heat treatment process. Meanwhile, an orthogonal experiment with four-factor three-level was designed, and the optimum heat treatment conditions for preparing LD glass-ceramics with excellent flexural strength were found. The order of influencing extent of heat treatment conditions is crystallization temperature > crystallization time > nucleation temperature > nucleation time. In addition, the crystallization behavior, phase formation, microstructure and flexural strength of glass were measured at different heat treatment temperatures. Remarkably, the optimal LD glass-ceramics sample has a strong flexural strength at 342 MPa, in which plentiful crystal grains with uniform and dense distribution are observed. These results indicate that micro-nano-LD whisker-reinforced glass-ceramics obtained by optimized heat treatment program offer a potential candidate for dental applications.

KEYWORDS

lithium disilicate, glass-ceramics, whisker, heat treatment, microstructure, flexural strength, orthogonal experiment

1 Introduction

As polyphase solid materials crystallizing in suitable glasses, the nucleation and crystal growth of glass-ceramics can be promoted by controlling the heat treatment process (Höland and Beall, 2002). Concentrated the advantages of ceramics and glasses, glass-ceramics have excellent light transmittance, aesthetics and biocompatibility, and mechanical properties have been significantly improved. Therefore, they play important roles in all-ceramic restorative materials as ideal oral aesthetic restorative materials. Recently, LD glass-ceramics were widely used in dental restoration, including veneers, inlays, onlays, single crowns and anterior three-unit fixed bridges, due to their superior mechanical properties compared with other types of glass-ceramics, such as leucite glass-ceramics and mica-type glass-ceramics and so on (Della

Bona and Kelly, 2008; Kern et al., 2012; Gehrt et al., 2013; Fu et al., 2020). However, the flexural strength of LD glass-ceramics is still much lower than that of zirconia, and the application in posterior and multi-unit fixed bridges is still limited (Tinschert et al., 2001; Esquivel-Upshaw et al., 2004; Makarouna et al., 2011).

In order to improve the strength of LD glass-ceramics for dental applications, extensive efforts had been done by adjusting the original composition or controlling the heat-treatment process. On one hand, LD glass-ceramics with high mechanical strength can be prepared by using TiO_2 and P_2O_5 as nucleating agents, which promote phase separation and crystallization (Khater and Idris, 2007). Al_2O_3 and K_2O doping in glass play a crucial role of glass network formers, modifiers and densification, resulting in well-densified and mechanically strong glass (Fernandes et al., 2010; 2014). Huang et al. prepared zirconia-toughened LD glass by adding 15 wt% tetragonal zirconia (3Y-TZP), which increased the mechanical properties to 340 MPa and 3.5 MPa·m$^{1/2}$ (Huang et al., 2014). However, the addition of heterogeneous phases (3Y-TZP) also had some adverse effects such as the difficulty of uniform distribution and the obstacle to densification (Zhang et al., 2019a). The introduction of micro-nano-LD whiskers in the LD glass system is an effective solution to the above problems. LD whiskers with nanometer and micro scale grown from single crystal can provide more crystallization sites, which is conducive to the formation of crystallization sites and further growth of crystals. The mechanical properties are greatly improved by compressive stress reinforcement, phase transformation and bridging toughening mechanisms (Zhang et al., 2019b; Zhao et al., 2021; Yan et al., 2022). On the other hand, heat treatment processes are most efficient for intensifying the performance by adjusting crystallization phases and microstructure, such as grain shape, grain size, and distribution (Sun et al., 2021). There are, however, few systematic studies on the heat treatment of micro-nano-LD whisker-reinforced glass-ceramics, which are essential data in the fabrication process.

In this paper, 3 wt% micro-nano-LD whiskers were added into the LD glasses, and the heat treatment process was optimized by orthogonal experiment to maximize the flexural strength of the glass-ceramics for the application of dental restorative materials. And the crystallization behavior, phase formation, microstructure and flexural strength at different heat treatment temperatures were also studied.

2 Materials and methods

2.1 Preparation of the micro-nano-LD whiskers

Micro-nano-LD whiskers were synthesized by hydrothermal method. $LiOH·H_2O$ and SiO_2 were mixed evenly as raw materials according to the molar ratio of Li/Si at 1, and soaked in deionized water for 4 h. Next, the solutions were placed in an autoclave and heated to 150°C holding for 6 h, followed by cooling to room temperature, centrifuging, washing, and finally dried at 80°C for 24 h to obtain the micro-nano LD whiskers.

2.2 Preparation of LD glass powders

Homogeneous mixture of 65.5SiO_2-27.5 Li_2O-1.2P_2O_5-2.0Al_2O_3-1.8K_2O-2.0La_2O_3 (in mol%) was melted in an

alumina crucible at 1,480°C for 2 h in air, then quickly quenched into deionized water to obtain the basic glasses. The basic glasses were dried, ground and then sieved to powders with particle size <48 μm for use.

2.3 DTA

Differential thermal analysis (DTA) measurements were performed on the powders composed of glass powders and the glass powders doped with 3 wt% whiskers using differential thermal analyser (HCT-4, Beijing Henven Instruments Co., Ltd., Beijing, Chain). Weighed powder samples (.1 g) were placed into alumina sample holders and an alumina standard was used as a reference material. The samples were tested from room temperature to 1,200°C at a rate of 10°C/min.

2.4 Blending and heat treatment of the glasses

The glass powders were doped with 3 wt% micro-nano-LD whiskers. Then the mixed powders were uniaxially pressed at 15 MPa in a hardened-steel die to produce cylindrical form. Then, the samples were sintered in a muffle furnace with different heat treatment process. Finally, the sintered products were cooled in the furnace to obtain the micro-nano-LD whisker-reinforced glass-ceramics.

2.5 Characterization

According to the standard of ISO 6872-2015, ten discs (12 mm × 2 mm) of glass-ceramics were prepared. The discs were ground to 1.2 ± .2 mm thickness and polished to a 3 μm finish using silicon carbide papers. The biaxial flexural strength was determined using a universal mechanical machine (UMT 6130, Shenzhen Suns Instruments Co., Ltd., Shenzhen, China) with a 1000 N load cell at a cross-head speed of 1 mm/min. The discs were placed at a support device with three steel balls on ring arrangement, and then load 1000 N at their centers at a cross-head speed of 1 mm/min. After fracture, the thickness of the discs was accurately measured with a digital caliper (Mitutoyo, Japan). The biaxial flexural strength is calculated using the following equation:

$$\sigma = -0.2387P(X-Y)/b^2$$
$$X = (1+\nu)\ln(r_2/r_3)^2 + [(1-\nu)/2](r_2/r_3)^2$$
$$Y = (1+\nu)[1+\ln(r_1/r_3)^2] + (1-\nu)(r_1/r_3)^2$$

Where σ is the maximum tensile stress, P is the measured load at fracture in Newtons, ν is the Poisson's ratio (set as .25 in ISO 6872), r_1 is the radius of support circle in mm, r_2 is the radius of loaded area in mm, r_3 is the radius of specimen in mm and b is the sample thickness in mm.

X-ray diffraction (XRD) analysis on the heat-treated glass-ceramic samples could be used to determine the crystalline of phases using a diffractometer (SmartLab, Riguka, Japan). The samples were ground into a powder, and X-ray diffraction analysis was performed with Cu-
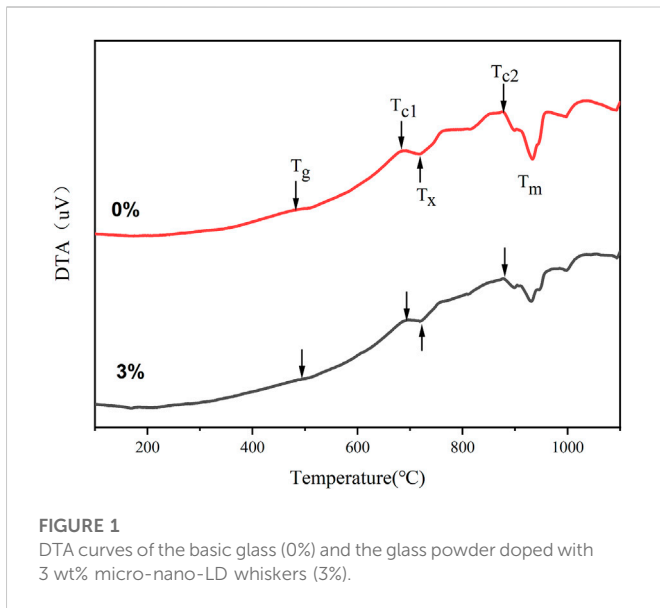
FIGURE 1
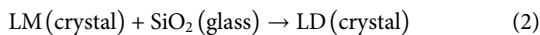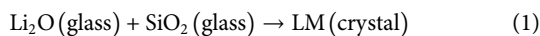DTA curves of the basic glass (0%) and the glass powder doped with 3 wt% micro-nano-LD whiskers (3%).

Kα radiation with the scanning speed of 2°/min under 40 kV and 30 mA working conditions. The XRD patterns were analyzed using MDI JADE software (version 6.0).

The size and morphology and quantity of the crystal phases in the samples were observed by scanning electron microscopy (SEM, Jeol JSM-7900F, Tokyo, Japan). Samples were prepared by cutting and polishing a section, which was then etched in 5 mass% HF for 30 s, cleaned with distilled water, coated with gold to make them conductive.

3 Results and discussions

3.1 DTA

As shown in Figure 1, two exothermic peaks are observed. A phase transition process from lithium metasilicate (Li_2SiO_3, referred as LM) to LD was generated by the increased temperature as the following equations (Wen et al., 2007):

$$Li_2O\,(glass) + SiO_2\,(glass) \rightarrow LM\,(crystal) \tag{1}$$

$$LM\,(crystal) + SiO_2\,(glass) \rightarrow LD\,(crystal) \tag{2}$$

Hence the two exothermic peaks in the DTA curves can be attributed to LM and LD crystallization respectively. And the peak temperatures are crystallization temperature, referred as T_{c1} and T_{c2}, respectively. T_x is the onset temperature of the crystallization of LD phase. The heat treatment temperature below T_m should be adopted to avoid the melting of LD glasses. The specific characteristic temperatures could be seen in Table 1.

For samples doped with 3 wt% whiskers (3%) compared to the basic glass (0%), T_{c1} increases from 687°C to 695°C, proving thus that the presence of whiskers inhibits the formation of LM. The glass transition temperature (T_g) gradually increases from 485°C to 491°C, while the temperature difference (ΔT_1) between T_g and T_x decreases from 234°C to 227°C, indicating that the crystallization ability is enhanced. At the same time, the temperature difference (ΔT_2) between T_{c2} and T_m is noted. The smaller ΔT_2 indicates a relatively narrow stable region and a more sensitivity to heat for the samples doped with 3% whiskers. Further, a two-peak structure could be suggested in the temperature region where LD crystallizes in the DTA curves. This may be an indication of the formation of a metastable LD precursor (Bischoff et al., 2011).

The dominant crystallization mechanism (surface or internal) was determined by DTA (Palou et al., 2009). The method considers $(\delta T)_p$, T_p and the ratio $T_p^2/(\Delta T)_p$ on the basic of DTA measurements, where $(\delta T)_p$ is the maximum height of the DTA peak, T_p is the temperature at $(\delta T)_p$, and $(\Delta T)_p$ is the peak half-width. For samples doped with 3 wt% whiskers (3%), decreasing value of $T_p^2/(\Delta T)_p$ implies the surface crystallization mechanism.

According to previous McMillan's claim, the optimal nucleation temperature is usually between T_g and higher than T_g 50°C (McMillan, 1997).

3.2 Results of orthogonal experiments

Based on previous DTA results in Figure 1 and Table 1, a four-factor three-level orthogonal experiments was designed to explore the respective effects of nucleation temperature, nucleation time, crystallization temperature, and crystallization time for optimizing the preparation process, as shown in Table 2. For samples from each group, the biaxial flexural strength was tested, and the average value was taken as the final result. The results of orthogonal experiments are presented in Table 3.

The influence of four factors evaluated using the range analysis approach is displayed in Figure 2. Where R, represented the range values, refers to the extreme difference of each factor, and the larger the range refers to the greater the influence of the factor on the flexural strength of the glass-ceramics. The range analysis of the orthogonal experiment elucidates the order of influence (from greatest to least) of the four factors affecting the flexural strength of the glass-ceramics: Factor C > Factor D > Factor A > Factor B. Remarkably, the optimal levels of A, B, C, and D are A2, B2, C3, D1, corresponding to nucleation temperature of 540°C, nucleation time of 1 h, crystallization temperature of 910°C, and crystallization time of .5 h. Under these conditions, the flexural strength of the glass-ceramics reaches at 342 MPa. R_C is 77.33, significantly higher than R_D, R_A, R_B, which are 16.67, 14.33 and 10.33, respectively. Therefore, crystallization temperature has the greatest effect on the flexural strength, while crystallization time, nucleation temperature and nucleation time have slight difference on it. The optimum

TABLE 1 DTA results of the basic glass (0%) and the glass powder doped with 3wt% whiskers (3%).

Sample (%)	T_g (°C)	T_{c1} (°C)	T_x (°C)	ΔT_1 (°C)	T_{c2} (°C)	T_m (°C)	ΔT_2 (°C)	$T_p^2/(\Delta T)_p$
0	485	687	719	234	875	933	58	4,846
3	491	695	718	227	877	930	53	5,128

TABLE 2 Orthogonal test table.

NO.	Factor A: Nucleation temperature (°C)	Factor B: Nucleation time (h)	Factor C: Crystallization temperature (°C)	Factor D: Crystallization time (h)
Level1	520	0.5	840	0.5
Level2	540	1	875	1
Level3	560	1.5	910	1.5

TABLE 3 Orthogonal Experiment Design and Corresponding mechanical properties Results.

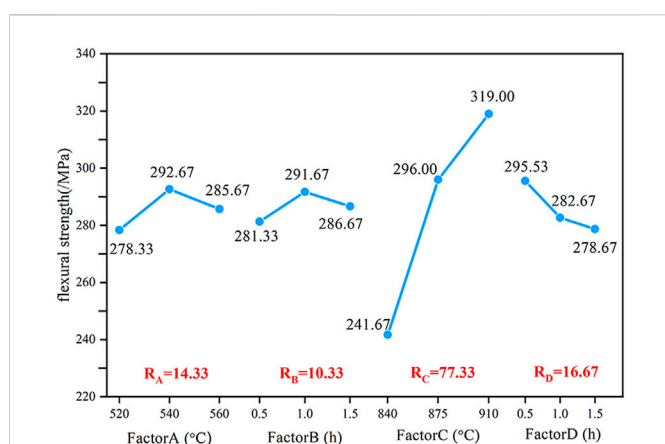| NO.	Factor A	Facto B	Factor C	Factor D	Biaxial flexural strength (MPa)
1	520	0.5	840	0.5	240
2	520	1	875	1	292
3	520	1.5	910	1.5	303
4	540	0.5	875	1.5	292
5	540	1	910	0.5	342
6	540	1.5	840	1	244
7	560	0.5	910	1	312
8	560	1	840	1.5	241
9	560	1.5	875	0.5	304

FIGURE 2
Influence of various factors on the compressive strength of glass-ceramics: (Factor A) nucleation temperature, (Factor B) nucleation time, (Factor C) crystallization temperature, and (Factor D) crystallization time.

nucleation temperature of 540°C (49°C above T_g = 491°C) are in agreement with the previous claim (McMillan, 1997).

3.3 Effects of heat treatment on microstructure and flexural strength

To investigate the mechanisms of heat treatment temperature factors from the standpoint of microstructural transformation, the properties of glass-ceramics in lithium silicate system were determined by controlled crystallization. Samples of glass-ceramics without LD whiskers and micro-nano-LD whisker-reinforced glass-ceramics with different crystallization temperatures were prepared by one-step heat treatment processes (Table 4).

As shown in Figure 3, the XRD patterns of the samples indicate the phase formations of glass-ceramic specimens incorporated different temperatures of heat treatment. There were four characteristic peaks representing the presence of four prominent crystalline phase of LM (PDF #29-0829), LD (PDF #40-0376), quartz (PDF #47-1144), lithium phosphate (Li_3PO_4, PDF #76-0556) and kalsilite ($KAlSiO_4$, PDF #76-0635). In W1, LM phases formed as the main phase could be determined after heat treatment at 700°C, while LD and $KAlSiO_4$ phases presented as the minor phases. In W2 treated at 840°C, the phases of LM and $KAlSiO_4$ were disappeared, which showed the main crystal phase for LD. When the temperature reached at 875°C and 910°C, a small amount of quartz and Li_3PO_4 phases were precipitated and the intensity of each diffraction peak gradually increased. In addition, well-defined diffraction patterns with sharp and robust diffraction peaks indicated a better precipitation and crystallinity of LD as heat treatment temperature increased. Compared to W0, W3 showed a similar diffraction peak pattern, and the intensity of the peaks was enhanced significantly, especially the peaks of LD crystals. It indicates that for W0 and W3, the two kinds of glass-ceramics with different composition under an identical preparation process, crystallinities of the samples are increased with the addition of micro-nano-LD whiskers.

The order of crystal precipitation is closely related to temperature (Headley and Loehman, 1984). P_2O_5 is added to the LD glass as

TABLE 4 Heat treatment processes of micro-nano-LD whisker-reinforced glass-ceramics.

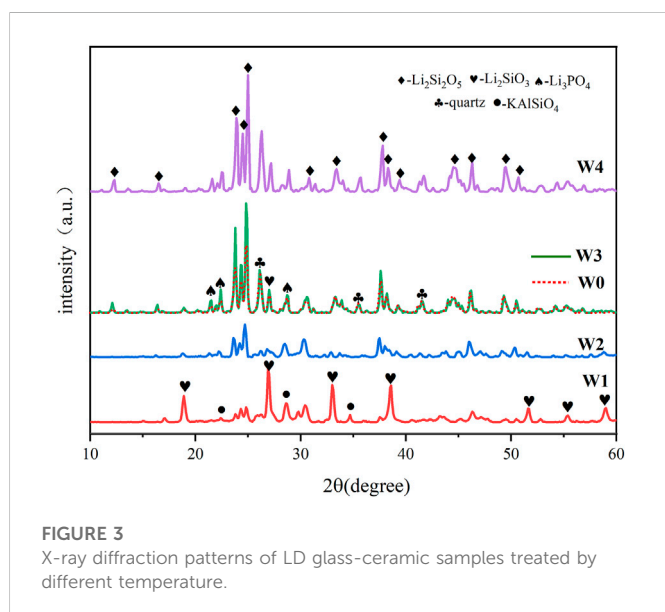| Sample	Crystallization temperature (°C)	Crystallization time (h)
W0	875	1
W1	700	1
W2	840	1
W3	875	1
W4	910	1

FIGURE 3
X-ray diffraction patterns of LD glass-ceramic samples treated by different temperature.

nucleating agent, which reduces the interfacial energy between the crystal nucleus and the glass matrix at the early period of crystallization. And then Li_3PO_4 transition phase containing Li forms subsequently, which is induced at the interface between the amorphous Li_3PO_4 and the glass matrix (Zheng et al., 2008, 5). As the temperature rises, LD crystals are generated due to the combination of LM and SiO_2, meaning, LM mesophases is formed before LD crystals (Iqbal et al., 1998; Bischoff et al., 2011).

At the temperature within the first exothermic peak of DTA (~700°C), LD was detected in addition to LM formation as main phase. The result was different from previous studies (Soares et al., 2015; Zhang et al., 2015; Kraipok et al., 2022), which LD could only be transformed from LM at higher temperature. Additionally, Li_3PO_4 was not detected because the amorphous form existed at low temperature, with less size and content (Höland et al., 2006; Sun et al., 2021). When the temperature increased to 840°C, the crystal phase of LM was unstable, and then LD formed and grew outwardly (Huang et al., 2013). The concomitant existence of Li_3PO_4 crystals and quartz could be a result of nucleation and growth on Li_3PO_4 nuclei and micro-nano-LD whiskers (Zhao et al., 2019). With the increase of temperature, LD phases of sample W1–W4 gradually increased, owing to the decrease in viscosity of glass and the increase mobility, which promoted the growth of crystal (Diaz-Mora et al., 1998). The detected minor $KAlSiO_4$ phase was due to the reaction between K, Al and SiO_2 in low temperature (below 840°C).

Figure 4 shows SEM images of the micro-nano-LD whiskers and LD glass-ceramics without whiskers after heat treatment at 875°C for 1 h. In Figure 4A, the whiskers were rod-like crystals with a length of .4–1.4 μm, a width of .05–.13 μm and the aspect ratio of 7–14. In Figure 4B, the specimens showed multi-directionally interlocked microstructure of numerous rod-like LD crystals protruding from the glass matrix, which the grain size and distribution of crystals were both uniform.

The SEM images of glass-ceramic samples treated by different temperature are demonstrated in Figure 5, which illustrates the influence of the temperature on microstructures of micro-nano-LD whisker-reinforced glass-ceramics. Figure 5A exhibited less dense, porous and mesh-like microstructure, in which a few small LD crystals scattered induced by whiskers after treated at 700°C. It revealed the crystallization induced by whiskers was still in an early stage combining the XRD results. At the same time, LM and Li_3PO_4 phases were not observed because they were highly soluble in HF acid solutions, and many voids could be seen in etched samples due to the dissolution of LM and Li_3PO_4 phases (Serbena et al., 2015; Li et al., 2016; Sun et al., 2021).

As shown in Figures 5B–D, rod-like LD crystals precipitated and formed multi-directionally interlocking microstructures. The crystal size gradually increased and the residual glass gradually decreased as the temperature increased. Additionally, it showed a bimodal crystal size distribution in which some larger grains with high aspect ratio embedded in a smaller grained matrix were observed.

Compared to W3, the grain size of W0 was more uniform and no larger grain was found, while crystallinity of W0 was not better than W3 according to the result of XRD. Consequently, considering the same thermal history, it can be concluded that in the compositions of W0 and W3 glass-ceramics, micro-nano-LD whisker is the main additive which causes the difference of crystallization mechanism between them. It can be believed a large number of fine short rod-like LD grains formed by the spontaneous surface nucleation of the glass powders and a small number of elongated rod-like crystals formed by whiskers epitaxial growth. Thus, the addition of whiskers as nucleating agent promotes heterogeneous crystallization of LD glass-ceramics. Whiskers are introduced to provide new nucleation sites for crystal formation, which induce crystallization process of LD with Li_3PO_4 together and greatly enhance the degree of crystallization (Yan et al., 2022). In addition, the addition of whiskers as a nucleating agent competes with Li_3PO_4 for the consumption of Li and Si, and thus inhibits the formation of LM.

When the temperature increased, the residual glass gradually decreased, and the crystal size of samples gradually increased both in the direction of length and width and apparently a small number of large grains appeared (Figures 5B–D). In Figure 6, the results showed
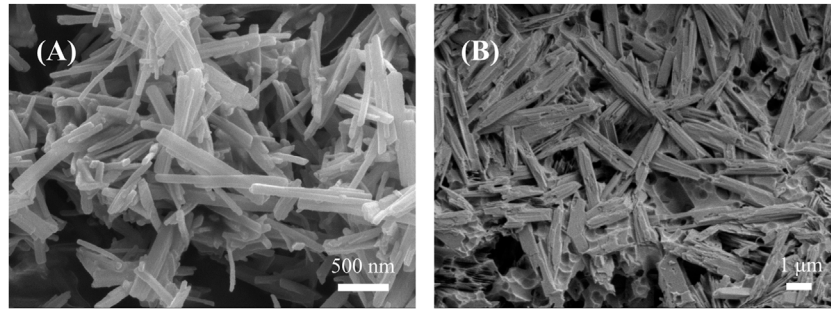
FIGURE 4
SEM images of micro-nano-LD whiskers **(A)** and sample W0 of LD glass-ceramics without whiskers **(B)**.
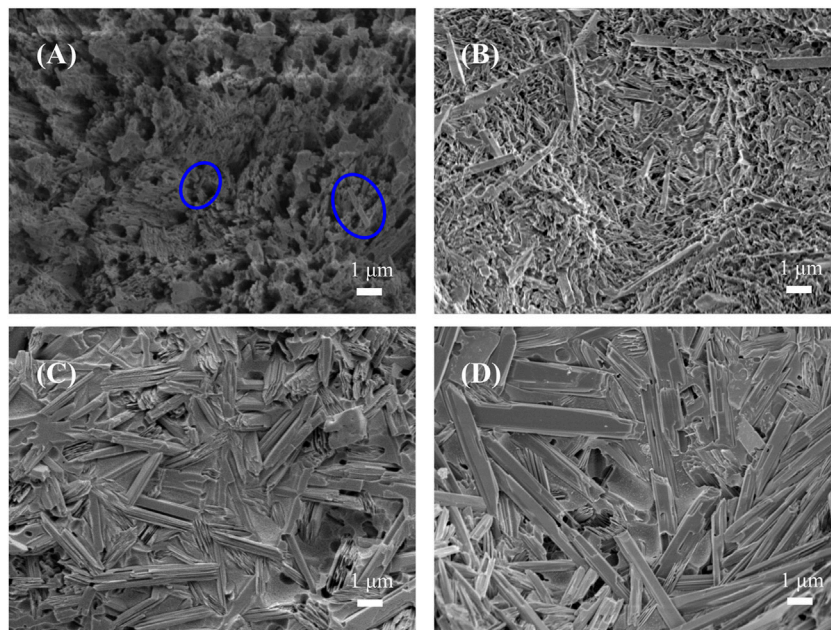

FIGURE 5
SEM images of LD glass-ceramics treated by different temperature: **(A)** W1; **(B)** W2; **(C)** W3; **(D)** W4.

the average length and width of the LD crystals increased from 1.36 to 4.02 μm and .31–.71 μm, respectively, and meanwhile, the average aspect ratio increased from 4.42 to 5.82.
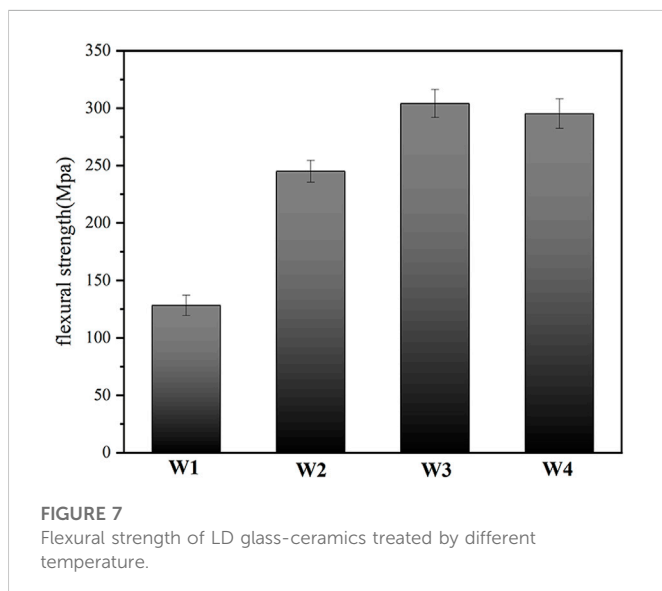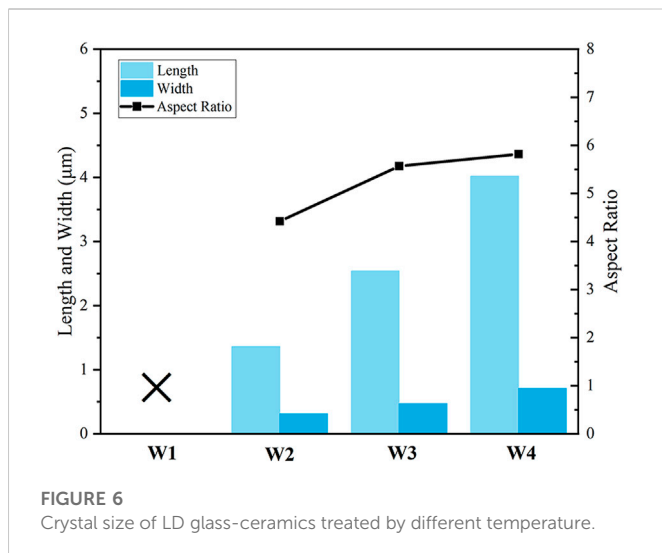
For glass system, viscosity is the main factor affecting the crystal growth rate. The higher the viscosity of the system lead to more difficult crystal growth and slower growth rate. The viscosity of the body system is mainly related to the temperature. The following Fulcher formula is usually used to describe them quantitatively (Diaz-Mora et al., 1998).

$$\log_{10} \eta = -A + B/(T - T_0)$$

η shows the viscosity of the body system, and A, B, T_0 are constant numbers associated with the body system. Accordingly with the increase of heat treatment temperature, viscosity of system reduces, and the crystal growth rate increases.

Figure 7 shows the flexural strength of micro-nano-LD whisker-reinforced glass-ceramics. The lowest flexural strength was found at 700 °C, owing to the porous structure of glass-ceramics with main phase of LM. However, it is also an advantage for dental materials using Computer-Aided Design/Computer-Aided Machining (CAD/CAM) milling, because the low strength glass-ceramics is more processable and can still achieve excellent properties by phase transition from LM to LD after secondary heat treatment (Xiang et al., 2020; Daguano et al., 2021). When the temperature reached to 840°C, the strength was greatly increased due to phase transformation from LM to LD.

As the temperature increased, the flexural strength could be enhanced by the increase crystal size and crystallization, which reached to the maximum of 304 MPa at 875°C. Interestingly, the flexural strength decreased slightly when the temperature reached to 910°C, though the size was larger and crystallization was better.

FIGURE 6
Crystal size of LD glass-ceramics treated by different temperature.

FIGURE 8
The SEM image of LD glass-ceramics treated by optimal heat treatment scheme (sample NO.5).

FIGURE 7
Flexural strength of LD glass-ceramics treated by different temperature.

This result can be interpreted that the flexural strength of glass-ceramics depends on interlocking effect and the residual stress effect. The interlocking effect is generated by the irregular distribution of rod-like crystals (Serbena et al., 2015). The residual stresses also exist in LD glass-ceramics due to the thermal expansion coefficient mismatch between the glass matrix and the crystals (Serbena and Zanotto, 2012). The average linear TECs of LD phase and the corresponding glass matrix are estimated to be $10.1–10.8 \times 10^{-6}/K$ and $12.2–12.8 \times 10^{-6}/K$, respectively. Residual compressive stresses inside the crystals along the radial direction and the balancing residual tensile stresses in the glass matrix along the tangential direction would exist at room temperature (Mastelaro and Zanotto, 1999; Pinto et al., 2007). When the crystal size increases, the interlocking effect is conducive to the enhancement of the flexural strength, but it is also accompanied by the increase of the residual stresses in the glass matrix. In the flexural strength test, the residual stress

overlaps with the macroscopic external tensile stress of the specimen, thus reducing the flexural strength (Li et al., 2016). Therefore, it is important to control the crystal size and avoid the abnormal crystal growth during heat treatment process. In this study, sample NO.5 showed a small and homogeneously distributed microstructure (Figure 8) formed by control of crystal size due to sufficient nucleation as the reason for the highest strength (342 MPa), which further proved the above conclusion. And at the optimal heat treatment of sample NO.5, the crystals had lengths and widths of 1.4–3.8 and .2–.6 μm, respectively. The small crystal formed by the crystallization of glass matrix reduces the residual stress, while the large crystal formed by the addition of whiskers increases the interlocking effect, thus realizing the mechanical enhancement. This is also the advantage of micro-nano-LD whisker-reinforced glass-ceramics.

4 Conclusion

A four-factor three-level orthogonal experiment design was used to optimize the heat treatment for preparing micro-nano-LD whisker-reinforced glass-ceramics. The orders that affect the flexural strength of glass-ceramics are the crystallization temperature > crystallization time > nucleation temperature > nucleation time. The optimal heat treatment scheme is determined as follows: nucleating at 540°C for 1 h and crystallizing at 910°C for .5 h. This scheme aims to improve the flexural strength of LD glass-ceramics and promote the applicability of restorative materials in dentistry.

With the increase of heat treatment temperature, LD gradually becomes the main crystalline phase, and the crystallinity increases, the crystal size increases, the residual glass decreases, and the flexural strength increases firstly and then slightly decreases.

The micro-nano-LD whisker-reinforced glass-ceramics produced with the optimal heat treatment system exhibited flexural strength up to 342 MPa. The large number of crystal grains, medium sizes, and uniform and compact distribution were the main reasons for improvement of the flexural strength of the glass-ceramics following process optimization.

Data availability statement

Author contributions

Funding

Acknowledgments

Conflict of interest

The authors declare that the research was conducted in the absence of any commercial or financial relationships that could be construed as a potential conflict of interest.

Publisher's note

All claims expressed in this article are solely those of the authors and do not necessarily represent those of their affiliated organizations, or those of the publisher, the editors and the reviewers. Any product that may be evaluated in this article, or claim that may be made by its manufacturer, is not guaranteed or endorsed by the publisher.

References

Bischoff, C., Eckert, H., Apel, E., Rheinberger, V. M., and Höland, W. (2011). Phase evolution in lithium disilicate glass–ceramics based on non-stoichiometric compositions of a multi-component system: Structural studies by 29Si single and double resonance solid state NMR. *Phys. Chem. Chem. Phys.* 13, 4540. doi:10.1039/c0cp01440k

Daguano, J. K. M. B., Dantas, L., Soares, V. O., Alves, M. F. R. P., Santos, C. dos, and Zanotto, E. D. (2021). Optimizing the microstructure of a new machinable bioactive glass-ceramic. *J. Mech. Behav. Biomed. Mat.* 122, 104695. doi:10.1016/j.jmbbm.2021.104695

Della Bona, A., and Kelly, J. R. (2008). The clinical success of all-ceramic restorations. *J. Am. Dent. Assoc.* 139, 8S–13S. 1939. doi:10.14219/jada.archive.2008.0361

Diaz-Mora, N., Zanotto, E. D., and Fokin, V. M. (1998). Crystal growth and viscous flow in cordierite and other glasses. *Phys. Chem. Glas.* 39, 91–97.

Esquivel-Upshaw, J. F., Anusavice, K. J., Young, H., Jones, J., and Gibbs, C. (2004). Clinical performance of a lithia disilicate-based core ceramic for three-unit posterior FPDs. *Int. J. Prosthodont.* 17, 469–475.

Fernandes, H. R., Tulyaganov, D. U., Goel, A., Ribeiro, M. J., Pascual, M. J., and Ferreira, J. M. F. (2010). Effect of Al2O3 and K2O content on structure, properties and devitrification of glasses in the Li2O–SiO2 system. *J. Eur. Ceram. Soc.* 30, 2017–2030. doi:10.1016/j.jeurceramsoc.2010.04.017

Fernandes, H. R., Tulyaganov, D. U., Pascual, M. J., and Ferreira, J. M. F. (2014). Structure–property relationships and densification-crystallization behaviours of simplified lithium disilicate glass compositions. *Ceram. Int.* 40, 129–140. doi:10.1016/j.ceramint.2013.05.113

Fu, L., Engqvist, H., and Xia, W. (2020). Glass-ceramics in dentistry: A review. *Mat. Basel Switz.* 13, E1049. doi:10.3390/ma13051049

Gehrt, M., Wolfart, S., Rafai, N., Reich, S., and Edelhoff, D. (2013). Clinical results of lithium-disilicate crowns after up to 9 years of service. *Clin. Oral Investig.* 17, 275–284. doi:10.1007/s00784-012-0700-x

Headley, T. J., and Loehman, R. E. (1984). Crystallization of a glass-ceramic by epitaxial growth. *J. Am. Ceram. Soc.* 67, 620–625. doi:10.1111/j.1151-2916.1984.tb19606.x

Höland, W., Apel, E., van 't Hoen, Ch., and Rheinberger, V. (2006). Studies of crystal phase formations in high-strength lithium disilicate glass–ceramics. *J. Non-Cryst. Solids* 352, 4041–4050. doi:10.1016/j.jnoncrysol.2006.06.039

Höland, W., and Beall, G. H. (2002). *Glass-ceramic technology.* Westerville, OH: American Ceramic Society.

Huang, S., Zhang, B., Huang, Z., Gao, W., and Cao, P. (2013). Crystalline phase formation, microstructure and mechanical properties of a lithium disilicate glass–ceramic. *J. Mat. Sci.* 48, 251–257. doi:10.1007/s10853-012-6738-y

Huang, X., Zheng, X., Zhao, G., Zhong, B., Zhang, X., and Wen, G. (2014). Microstructure and mechanical properties of zirconia-toughened lithium disilicate glass–ceramic composites. *Mat. Chem. Phys.* 143, 845–852. doi:10.1016/j.matchemphys.2013.10.023

Iqbal, Y., Lee, W. E., Holland, D., and James, P. F. (1998). Metastable phase formation in the early stage crystallisation of lithium disilicate glass. *J. Non-Cryst. Solids* 224, 1–16. doi:10.1016/S0022-3093(97)00453-5

Kern, M., Sasse, M., and Wolfart, S. (2012). Ten-year outcome of three-unit fixed dental prostheses made from monolithic lithium disilicate ceramic. *J. Am. Dent. Assoc.* 143, 234–240. 1939. doi:10.14219/jada.archive.2012.0147

Khater, G. A., and Idris, M. H. (2007). Role of TiO2 and ZrO2 on crystallizing phases and microstructure in Li, Ba aluminosilicate glass. *Ceram. Int.* 33, 233–238. doi:10.1016/j.ceramint.2005.08.016

Kraipok, A., Intawin, P., Bintachitt, P., Leenakul, W., Khamman, O., Eitssayeam, S., et al. (2022). Influence of heat treatment temperature on the properties of the lithium disilicate-fluorcanasite glass-ceramics. *Int. J. Appl. Ceram. Technol.* 19, 1415–1427. doi:10.1111/ijac.13945

Li, D., Guo, J. W., Wang, X. S., Zhang, S. F., and He, L. (2016). Effects of crystal size on the mechanical properties of a lithium disilicate glass-ceramic. *Mat. Sci. Eng. A* 669, 332–339. doi:10.1016/j.msea.2016.05.068

Makarouna, M., Ullmann, K., Lazarek, K., and Boening, K. W. (2011). Six-year clinical performance of lithium disilicate fixed partial dentures. *Int. J. Prosthodont.* 24, 204–206.

Mastelaro, V. R., and Zanotto, E. D. (1999). Anisotropic residual stresses in partially crystallized Li2O–2SiO2 glass-ceramics. *J. Non-Cryst. Solids* 247, 79–86. doi:10.1016/S0022-3093(99)00038-1

McMillan, P. W. (1997). *Glass-ceramics.* London: Academic Press.

Palou, M., Kuzielová, E., Vitkoki, M., Lutianová, G., and Noaman, M. (2009). Transformation of glass to glass-ceramics in LiO2-SiO2 system. *Ceram. Silik.* 53.

Pinto, H., Ito, L., Crovace, M., Ferreira, E. B., Fauth, F., Wroblewski, T., et al. (2007). Surface and bulk residual stresses in Li2O·2SiO2 glass–ceramics. *J. Non-Cryst. Solids* 353, 2307–2317. doi:10.1016/j.jnoncrysol.2007.04.007

Serbena, F. C., Mathias, I., Foerster, C. E., and Zanotto, E. D. (2015). Crystallization toughening of a model glass-ceramic. *Acta Mater* 86, 216–228. doi:10.1016/j.actamat.2014.12.007

Serbena, F. C., and Zanotto, E. D. (2012). Internal residual stresses in glass-ceramics: A review. *J. Non-Cryst. Solids* 358, 975–984. doi:10.1016/j.jnoncrysol.2012.01.040

Soares, R. S., Monteiro, R. C. C., Lima, M. M. R. A., and Silva, R. J. C. (2015). Crystallization of lithium disilicate-based multicomponent glasses - effect of silica/lithia ratio. *Ceram. Int.* 41, 317–324. doi:10.1016/j.ceramint.2014.08.074

Sun, Y., Ma, L., Cui, J., Feng, L., Zhang, Z., Yang, Y., et al. (2021). Effects of heat-treatment temperature and holding time on the microstructure and mechanical properties of lithium disilicate glass-ceramics. *J. Non-Cryst. Solids* 553, 120502. doi:10.1016/j.jnoncrysol.2020.120502

Tinschert, J., Natt, G., Mautsch, W., Augthun, M., and Spiekermann, H. (2001). Fracture resistance of lithium disilicate-alumina-and zirconia-based three-unit fixed partial dentures: A laboratory study. *Int. J. Prosthodont.* 14, 231–238. doi:10.1038/sj.dmfr.4600604

Wen, G., Zheng, X., and Song, L. (2007). Effects of P2O5 and sintering temperature on microstructure and mechanical properties of lithium disilicate glass-ceramics. *Acta Mater* 55, 3583–3591. doi:10.1016/j.actamat.2007.02.009

Xiang, Z.-X., Chen, X.-P., Song, X.-F., and Yin, L. (2020). Responses of pre-crystallized and crystallized zirconia-containing lithium silicate glass ceramics to diamond machining. *Ceram. Int.* 46, 1924–1933. doi:10.1016/j.ceramint.2019.09.170

Yan, J., Liu, X., Wu, X., Wu, X., Zhang, Y., and Li, B. (2022). Microstructure and mechanical properties of Li2Si2O5 whisker-reinforced glass-ceramics. *Front. Mat.* 9, 849601. doi:10.3389/fmats.2022.849601

Zhang, H., He, Z., Zhang, Y., Jing, W., Wang, B., and Yang, J. (2015). Lithium disilicate glass-ceramics by heat treatment of lithium metasilicate glass-ceramics obtained by hot pressing. *J. Am. Ceram. Soc.* 98, 3659–3662. doi:10.1111/jace.13950

Zhang, F., Reveron, H., Spies, B. C., Van Meerbeek, B., and Chevalier, J. (2019a). Trade-off between fracture resistance and translucency of zirconia and lithium-disilicate glass ceramics for monolithic restorations. *Acta Biomater.* 91, 24–34. doi:10.1016/j.actbio.2019.04.043

Zhang, H., Wang, J., and Yang, J. (2019b). Anisotropic growth and photoluminescence of Li2Si2O5 hydrate rods. *J. Mat. Sci. Mat. Electron.* 30, 17405–17411. doi:10.1007/s10854-019-02090-6

Zhao, T., Li, A.-J., Qin, Y., Zhu, J.-F., Kong, X.-G., and Yang, J.-F. (2019). Influence of SiO2 contents on the microstructure and mechanical properties of lithium disilicate glass-ceramics by reaction sintering. *J. Non-Cryst. Solids* 512, 148–154. doi:10.1016/j.jnoncrysol.2019.02.015

Zhao, T., Lian, M.-M., Qin, Y., Zhu, J.-F., Kong, X.-G., and Yang, J.-F. (2021). Improved performances of lithium disilicate glass-ceramics by seed induced crystallization. *J. Adv. Ceram.* 10, 614–626. doi:10.1007/s40145-021-0463-4

Zheng, X., Wen, G., Song, L., and Huang, X. X. (2008). Effects of P2O5 and heat treatment on crystallization and microstructure in lithium disilicate glass ceramics. *Acta Mater* 56, 549–558. doi:10.1016/j.actamat.2007.10.024